

Homodyne chiral polarimetry for measuring thermo-optic refractive index variations

RUEY-CHING TWU* AND JHAO-SHENG WANG

Department of Electro-Optical Engineering, Southern Taiwan University of Science and Technology, No. 1 Nan-Tai Street, Yung Kang, Tainan 71005, Taiwan

*Corresponding author: rctwu@mail.stust.edu.tw

Received 1 May 2015; revised 9 September 2015; accepted 11 September 2015; posted 14 September 2015 (Doc. ID 239805); published 8 October 2015

Novel reflection-type homodyne chiral polarimetry is proposed for measuring the refractive index variations of a transparent plate under thermal impact. The experimental results show it is a simple and useful method for providing accurate measurements of refractive index variations. The measurement can reach a resolution of 7×10^{-5} . © 2015 Optical Society of America

OCIS codes: (120.5050) Phase measurement; (120.5410) Polarimetry; (130.3730) Lithium niobate; (130.6010) Sensors.

<http://dx.doi.org/10.1364/AO.54.008747>

1. INTRODUCTION

The refractive index (RI) of a transparent medium is an essential parameter for the fabrication of optical devices. The RI is dependent on the environmental conditions, especially thermal impacts. The study of thermo-optic (TO) effects is important for nonlinear-optic solid-state lasers, polymeric thermo-optic waveguide switches, and optical projectors [1–3]. Recently, transparent plates (TPs) have been widely used in various smart phones and other displays. Low TO sensitivity is necessary to obtain long-term image stability [3]. To measure the RI, the transmission and reflection arrangements can be performed in a common-path or a splitting-path interferometer using heterodyne interferometry [4,5].

In this paper, novel homodyne chiral polarimetry (HCP) is proposed to measure RI variations based on an external reflection concept. In the external reflection, there is no phase delay between both orthogonal polarizations when the incident angle is less than the Brewster's angle, which means that typical polarimetry cannot be used to measure the RI under the external reflection. However, the ratio changes between two orthogonal polarizations of reflected light will cause the azimuth angle to change. This behavior is similar to that of linearly polarized light passing through a chiral medium, and the changes of the azimuth angle are dependent on the activity and propagation length [6]. The azimuth angle changes can be converted into a phase delay between orthogonal polarizations in the circular polarimetric interferometer [6]. Therefore, circular polarimetric interferometers have been widely used for the measurements of chiral liquid concentrations and roll angular displacements [6,7]. In conventional circular polarimetry, the amplitudes of the circular polarization traces are nearly equal.

In our previous work [8], homodyne interferometry could only be used to measure the phase delay between orthogonal polarizations, as even the amplitudes of both polarizations changed during the measurement periods. According to the reflectance principle, the azimuth angles are dependent on the incident angle and relative index between different boundaries. At the same incident angle, the polarization traces of the reflected light are spiral-like along the propagation path under different relative RIs. The proposed HCP, which combines the measurement concepts of homodyne and circular polarimetry, has been evaluated and the accuracy of the measurements of the RI variations of the TP by measuring the phase variations demonstrated.

2. MEASUREMENT SETUP AND PRINCIPLE

Figure 1 illustrates the experimental arrangement for a refractive index variation measurement of the TP based on the HCP.

The illumination light, provided by an He–Ne laser (632.8 nm), is passed through a polarizer (PL) and a half-wave plate (HWP). Then, the light with both orthogonal polarizations is coupled into a lithium niobate Zn-indiffused phase modulator (ZIPM) through an objective lens (L1). The home-made ZIPM is a waveguide-type electro-optic device which was fabricated in an x-cut/z-propagation lithium niobate substrate. The detailed fabrication process has been reported in [8]. The width of the waveguide was 4 μm . The length and gap-width of the parallel electrodes were 12 mm and 14 μm , respectively. Compared to a commercial buck-type electro-optic modulator (Model 4002, New Focus, Inc.), the ZIPM has a lower driving voltage and smaller phase variation as reported in [9]. The homodyne light is generated by applying a sinusoidal voltage

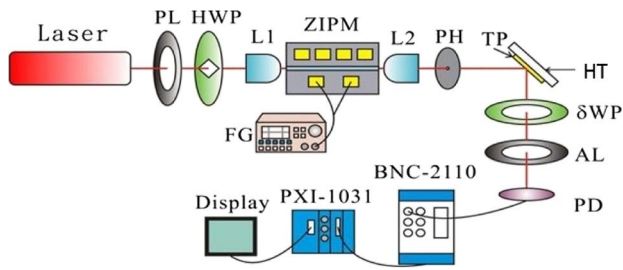


Fig. 1. Schematic diagram of a homodyne chiral polarimetric interferometer.

on the ZIPM from a function generator (FG). The output light from the ZIPM is then focused through another objective lens (L2). The scattering light is filtered out through a pinhole (PH). The sensing light propagates into the tested TP attached to a hot plate (HT). The reflected light from the TP passes a half-wave plate (δ WP), an analyzer (AL), and is received by a photodetector (PD). The converted electrical signal is sent to a signal acquisition box (BNC-2110) and analyzed with a fast Fourier transformation scheme in a LabVIEW platform (PXI-1031) [8]. For the incident orthogonal polarizations (p - and s -waves) with the same intensity, the reflectance of both polarizations are represented by R_p and R_s [10] as

$$R_p = \left(\frac{n_i \cos \theta_t - n_{tp} \cos \theta_i}{n_i \cos \theta_t + n_{tp} \cos \theta_i} \right)^2, \quad (1)$$

$$R_s = \left(\frac{n_i \cos \theta_i - n_{tp} \cos \theta_t}{n_i \cos \theta_i + n_{tp} \cos \theta_t} \right)^2, \quad (2)$$

where n_i and n_{tp} are the RIs of the incident space and the TP, respectively. θ_i and θ_t are the incident and the refracted angles, respectively. In a case where the incident angle is less than the Brewster's angle, there is no phase delay between the p - and s -polarizations. The reflection-induced azimuth angle is defined as

$$\beta = \tan^{-1} \left(-\sqrt{R_s/R_p} \right). \quad (3)$$

In the proposed CPI, the phase variations of the reflected light due to the change of the azimuth angle are represented as [6]

$$\phi_{TP} = \tan^{-1} \left[\tan \frac{1}{2} \delta (\cos 2(\Delta\beta + \alpha) + \sin 2(\Delta\beta + \alpha)) \right] - \tan^{-1} \left[\tan \frac{1}{2} \delta (\cos 2(\Delta\beta + \alpha) - \sin 2(\Delta\beta + \alpha)) \right], \quad (4)$$

where δ and α are the phase retardation and roll angle of δ WP, respectively. In the common-path polarization interferometer, the phase variations between two orthogonal polarizations can be obtained by utilizing the reported homodyne interferometry [8].

3. SIMULATION AND EXPERIMENTAL RESULTS

Typically, the refractive indices of commercial crown glass are in the range of 1.51–1.55 refractive index units (RIUs), which

are also wavelength dependent. These values were chosen for the calculations. The reflectance of the p -wave was decreased gradually to zero as the incident angle close to the Brewster's angle. At the same time, the variation of the azimuth angle was enhanced. However, the signal fluctuation is increased due to the noise impact from the low reflectance signal. It is necessary to optimize the incident angle. When the reflectance of the p -wave was equal to zero, its Brewster's angle was about 56.5° at the TP's RI of 1.51 in free space. The simulated incident angles were below 56.5° . A comparison of the azimuth angle variations versus the RIs of the TP for different incident angles is shown in Fig. 2(a). The azimuth angle decreased negatively as the RI of the TP increased. The differences in the azimuth angles are summarized in Fig. 2(b). The slope of the azimuth angle versus the RI was dependent on the incident angle. Of the simulated angles, the incident angle 45° had the maximum ratio.

According to Eq. (4), the dependence of the phase variation on the roll angle change close to the most sensitive region for various RIs of the TP is shown in Fig. 3. The step-like phase change was achievable at a δ close to 180° . The curves showed a left shift with the increase of the RI of the TP due to a positive increase in the azimuth angle. It means that the phase variation caused by the RI change of the TP can be observed easily at a specific roll angle.

Figure 4 illustrates the phase variation versus refractive index of the TP for the different α and δ of the δ WP. The measurement sensitivity is represented by the slope of the phase versus the RI. According to the simulations, the sensitivity and dynamic range of the phase versus the RI changes were dependent

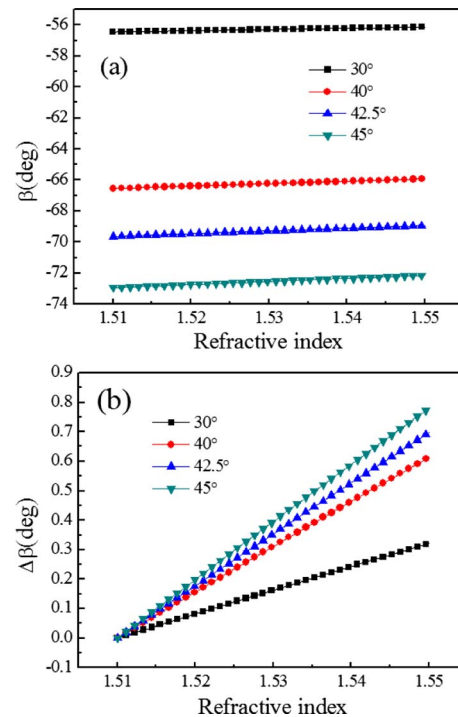


Fig. 2. (a) Azimuth angle difference versus refractive index of the TP for different incident angles. (b) Difference of the azimuth angle based on an initial RI of 1.51 for different incident angles.

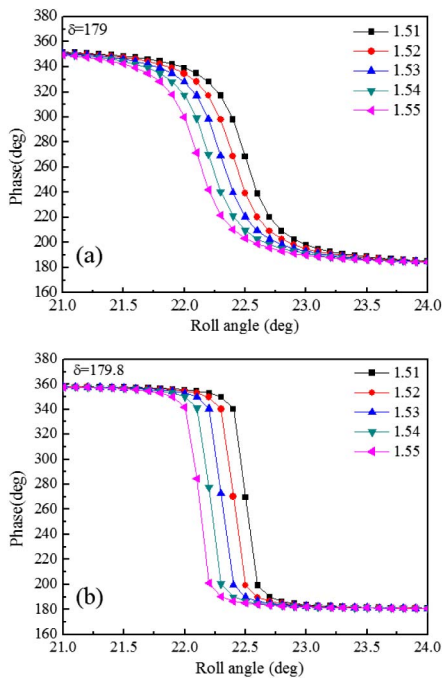


Fig. 3. Phase variation versus roll angle change for various refractive indices of the TP: (a) $\delta = 179^\circ$ and (b) $\delta = 179.8^\circ$.

on the chosen δ and initial roll angle α of the δ WP. When δ was 179.8° and α was 22.4° or 22.5° , the phase variation was 70 deg under an RI changing from 1.51 to 1.52, as shown in Figs. 4(a) and 4(b). Therefore, the best sensitivity value was 7×10^3 . The expected sensitivity values were larger than 7×10^3 at δ equal to 180° .

To evaluate the proposed methodology for real applications, a BK-7 glass plate 2 mm in thickness (RI = 1.51) was placed on the hot plate. The RI increased as the temperature of the hot plate increased due to the positive thermo-optic coefficient of the glass. From the simulation results (Fig. 4), it is observed that the sensitivity and dynamic range is deeply dependent on the initial roll angle of the δ WP. Before measuring the temperature-dependent phase variation, the most sensitive roll angle was decided by rotating the δ WP for a period of 90 deg. The initial roll angle was chosen at the angle with an abrupt phase change. The temperature increased gradually from an ambient temperature of 30°C to the heating temperature of 100°C within 2 min, where it stayed for 2 min, and then the heater power was turned off to allow for natural cooling. The phase variation versus time under the temperature changes is shown in Fig. 5. An increase in temperature will result in an increase of RI of the TP. The trend of the decreased phase variation was in good agreement with the simulation results, as shown in Fig. 4. The phase variation trace was similar to the temperature variation (red dotted line). The phase difference was 3 deg for a temperature change of 70°C . The phase stability was around 1 deg. The calculated RI change is 2.1×10^{-4} RIU by considering the thermo-optic coefficient of around 3×10^{-6} ($1/^\circ\text{C}$) [11]. The measurement sensitivity was 1.4×10^4 and the measurement of the refractive index variation reached a resolution of 7×10^{-5} RIU.

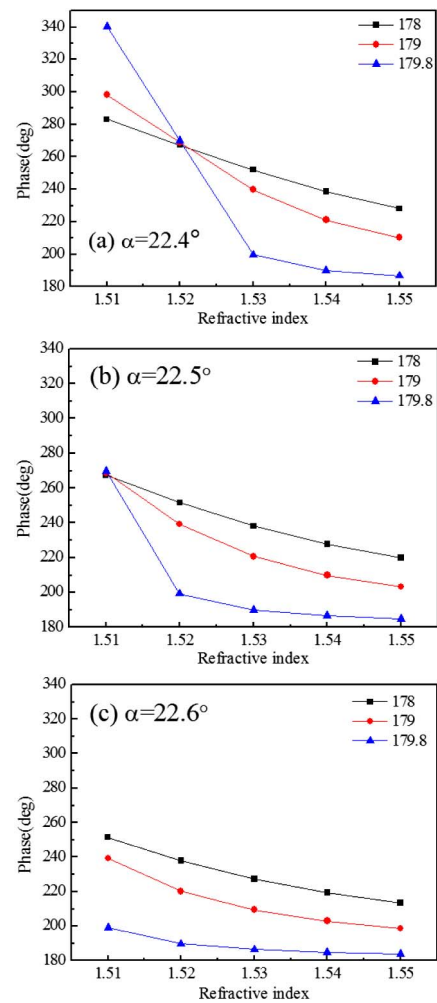


Fig. 4. Phase versus refractive index of the TP for different δ of δ WP: (a) initial roll angle α at 22.4° , (b) 22.5° , and (c) 22.6° .

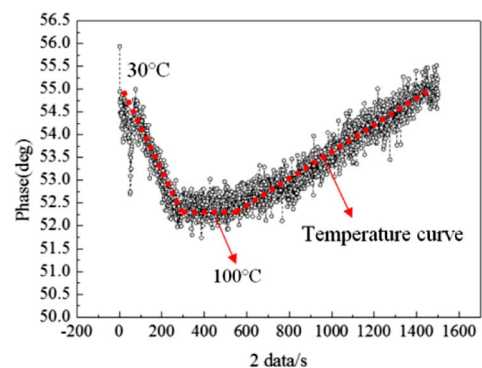


Fig. 5. Phase variations under the temperature changes.

4. CONCLUSION

In conclusion, simple reflection-type homodyne chiral polarimetry was proposed to measure the thermo-optic refractive index variations of a transparent plate. The simulation and experimental results showed that it could provide enough measurement sensitivity and fine resolution.

Funding. Ministry of Science and Technology, Taiwan (MOST) (MOST 103-2221-E-218-004).

REFERENCES

1. D. J. Ripin, J. R. Ochoa, R. L. Aggarwal, and T. Y. Fan, "165-W cryogenically cooled Yb:YAG laser," *Opt. Lett.* **29**, 2154–2156 (2004).
2. X. B. Wang, J. Sun, Y. F. Liu, J. W. Sun, C. M. Chen, X. Q. Sun, F. Wang, and D. M. Zhang, "650-nm 1×2 polymeric thermo-optic switch with low power consumption," *Opt. Express* **22**, 11119–11128 (2014).
3. A. F. Kurtz and J. R. Biety, "Lens design with reduced sensitivity to thermally induced stress birefringence," *Appl. Opt.* **52**, 4311–4322 (2013).
4. C. C. Hsu, S. Y. Chen, and Y. C. Chen, "Measuring the refractive index of transparent materials using high precision circular heterodyne interferometry," *Opt. Laser Eng.* **50**, 1689–1693 (2012).
5. M. H. Chiu, J. Y. Lee, and D. C. Su, "Refractive-index measurement based on the effects of total internal reflection and the uses of heterodyne interferometry," *Appl. Opt.* **36**, 2936–2939 (1997).
6. C. M. Wu and T. T. Chuang, "Roll angular displacement measurement system with microradian accuracy," *Sens. Actuators A* **116**, 145–149 (2004).
7. J. Y. Lin and D. C. Su, "A new method for measuring the chiral parameter and the average refractive index of a chiral liquid," *Opt. Commun.* **218**, 317–323 (2003).
8. R. C. Twu, H. Y. Hong, and H. H. Lee, "An optical homodyne technique to measure photorefractive-induced phase drifts in lithium niobate phase modulators," *Opt. Express* **16**, 4366–4374 (2008).
9. R. C. Twu, Y. H. Lee, and H. Y. Hou, "A comparison between two heterodyne light sources using different electro-optic modulators for optical temperature measurements at visible wavelengths," *Sensors* **10**, 9609–9619 (2010).
10. E. Hecht, *Optics*, 4th ed. (Addison-Wesley, 2002).
11. G. Ghosh, "Sellmeier coefficients and dispersion of thermo-optic coefficients for some optical glasses," *Appl. Opt.* **36**, 1540–1546 (1997).